Hindawi
Complexity
Volume 2022, Article ID 6595314, 17 pages
https://doi.org/10.1155/2022/6595314

Research Article

Robustness Analysis of the Regional and Interregional Components of the Weighted World Air Transportation Network

Issa Moussa Diop,[1] **Cherif Diallo**,[1] **Chantal Cherifi**,[2] **and Hocine Cherifi**[3]

[1]*Lacca Lab, Gaston Berger University, Saint-Louis, Senegal*
[2]*Disp Lab, University of Lyon 2, Lyon, France*
[3]*Lib Ea 7534, University of Burgundy Franche-Comté, Dijon, France*

Correspondence should be addressed to Issa Moussa Diop; diop.issa-moussa@ugb.edu.sn

Received 29 July 2022; Accepted 20 October 2022; Published 3 November 2022

Academic Editor: May T. Lim

Copyright © 2022 Issa Moussa Diop et al. This is an open access article distributed under the Creative Commons Attribution License, which permits unrestricted use, distribution, and reproduction in any medium, provided the original work is properly cited.

The robustness of a system indicates its ability to withstand disturbances while maintaining its properties, performance, and efficiency. There are plenty of studies on the robustness of air transport networks in the literature. However, few works consider its mesoscopic organization. Building on the recently introduced component structure, we explore the impact of targeted attacks on the weighted world air transportation network on its components. Indeed, it contains five local components covering different regions (North America-Caribbean, Europe-Russia, East and Southeast Asia-Oceania, Africa-Middle East-Southern Asia, and South America) and one global component linking these regions. We investigate targeted attacks based on influential weighted centrality measures (strength, betweenness, and PageRank). Results show that the local components gradually separate from the world air transportation network as the fraction of removed airports grows. The weighted betweenness attack removes fewer top airports to isolate the regions compared to its alternatives. Furthermore, it is still convenient to travel locally in the separate areas. In contrast, strength and PageRank attacks need to target more airports to split the network. However, they are more disruptive. Indeed, the size of the isolated local components reduces drastically, so it becomes more challenging to travel locally. Looking at the world air transportation network through its component structure reveals a new viewpoint on its resilience. It opens new perspectives to design more efficient attacks.

1. Introduction

The air transportation network is essential for the development and integration of countries. Indeed, millions of people and tons of frets from different world regions pass through the air. Ensuring secure and effective air transport infrastructure and traffic is a vital issue. The complex network paradigm allows for a better understanding of an extensive range of complex in-interconnected systems such as infrastructure, economics, and social networks [1]. Considering the air transportation networks where nodes represent airports and links are flights between two airports, network robustness is a popular tool to study the response to possible disruptions. Disruptions can be accidents or intentional attacks on airports or flights. Numerous investigations on the robustness of air transport networks (worldwide, regional, and national airlines) have been conducted [2–7]. In the following paragraph, we concentrate on targeted attacks based on centrality measures. It consists in ranking the airports according to a given centrality measure and removing the nodes in the descending order of their centrality value. The following paragraph summarizes some important related works.

In [8], the authors explore the robustness of the global air transportation network. They investigate five centrality measures (degree, betweenness, modal analysis, damage, and Bonacich power). They measure the effectiveness of the attacks using the size of the largest connected component (LCC). Indeed, the attacks split the network into multiple components. Results show that damage is most effective

when a small proportion of airports are attacked (<2.5%). Beyond this value, betweenness takes the lead. The other strategies are less effective. Indeed, modal analysis is good when more than 10% of airports are isolated. For larger fractions of isolated airports, Bonacich power outperforms degree. In [9], the authors investigate the robustness of the directed and weighted world air transportation network. Besides the unweighted network, they consider two weighting schemes: the geographical distances and the number of passengers traveling between two airports. They evaluate six targeted attacks based on various centralities ordered in descending and ascending order (strength, betweenness, closeness, eigenvector, damage, and Bonacich). Moreover, three metrics (unaffected passenger with rerouting, survival links, and size of the largest connected component) quantify the robustness. The unaffected passenger with rerouting is a baseline measure. The survival link measure introduced in this paper is the proportion of remaining links. The correlation analysis between these metrics shows that the unaffected passengers with rerouting and survival links are well correlated. The world air transportation network is more sensitive to attacks based on Bonacich and degree. Attacks are more effective when one takes into account the number of passengers.

Numerous airports and routes have been disrupted during the COVID-19 pandemic. In [10], the authors explore the impact of the first wave on the structure of the global air network and the epidemic spreading. They consider a network where nodes are cities and links are flights between the cities. They observe that the average distance between airports increases and long-distance flights decrease. The average betweenness and the number of triangles also drop significantly. They show that one can simulate this situation using a mixture of random and degree-based attacks. Furthermore, they show that politically motivated shutdowns lead to high variations in airport centrality and have consequences on national and international economies. Finally, the global air transport network started recovering its initial structure when the situation returned to normal.

In [11], the authors investigate the resilience of eight weighted domestic air transportation networks (Russia, Brazil, Australia, Canada, India, China, the US, and European). The number of routes is the weight of each of these networks. The attacks target the airports according to the decreasing order of their local weighted efficiency measures. The global weighted efficiency measures the robustness of the networks. They show that airports with high weighted efficiency have a large degree and strength. Moreover, two groups of domestic air transportation networks appear. The first, including Australia, Canada, India, and the US, are the most vulnerable. Indeed, removing 5% of the most critical airports reduces the weighted efficiency to 70%. The second groups, including the other air transportation networks, are more resilient. Indeed, removing the same proportion of airports in these networks reduces only 40% of their weighted efficiency.

In [12], the authors explore the robustness of the Northeast Asian network (China, Japan, and South Korea). They use three types of networks, one unweighted and two weighted (distance and link-wise air traffic). Targeted attacks rely on six centrality measures (degree, betweenness, closeness, strength, weighted betweenness, and weighted closeness). Evaluation includes two robustness metrics (the size of the largest connected component and the number of operable flights with optional rerouting). The Northeast Asia network is seriously affected when the weighted betweenness attack concerns 0.8% of airports. Indeed, its size decreases to around 50%. According to betweenness, the same damage is detected when targeting the top 2% of airports. There is a considerable gap in operable flights if one considers rerouting or not for all the weighted attacks. In [5], the authors study the robustness of the air transportation network of the belt and road regions. Nodes are cities that contain an airport with more than 25 airlines and the country capitals. The number of flights between two destinations represents the weights in the network. Targeted attack strategies use recursive power and recursive centrality. The efficiency measure assesses the impact of the attacks. In addition, the authors define an edge addition strategy to improve the network efficiency. Results show that attacks based on recursive power are the most effective. In addition, adding links with top recursive power nodes increase the network's robustness.

Our work departs from these studies. Indeed, we analyze the resilience of the weighted world air transportation network from a new viewpoint centered on the component structure. Previous work shows that the local components correspond to delimited geographical, economic, and cultural areas. In contrast, the global components represent their interactions and cover the world [13]. Therefore, this study also concerns various local regions of the world. However, the attacks are not local. They target the entire world air transportation network independently of its component structure. It allows for investigating the impact of targeted attacks worldwide on the different regional infrastructures. It shows that a high level of perturbations on the world air transportation network does not necessarily translate to poor travel experience at the regional level. A preliminary work is reported in [14].

The rest of the paper is organized as follows: the section briefly introduces the basic elements of this study. The section presents the data and methods. The section analyzes the component structure. The section reports the main findings on the strength attack. The section evaluates the weighted betweenness attack. The section assesses the weighted PageRank attack. The section discusses the results. Finally, the section concludes the study.

2. Background

2.1. Component Structure. The component structure attempts to capture the dense parts of the network. Indeed, in real-world networks, the density is inhomogeneous. The community [15–17] and core-periphery [18, 19] structures are good features to capture this phenomenon. Indeed, communities are dense clusters of nodes loosely connected. Cores are also dense parts of the multicore-periphery structure [19]. Peripheral nodes with few connections

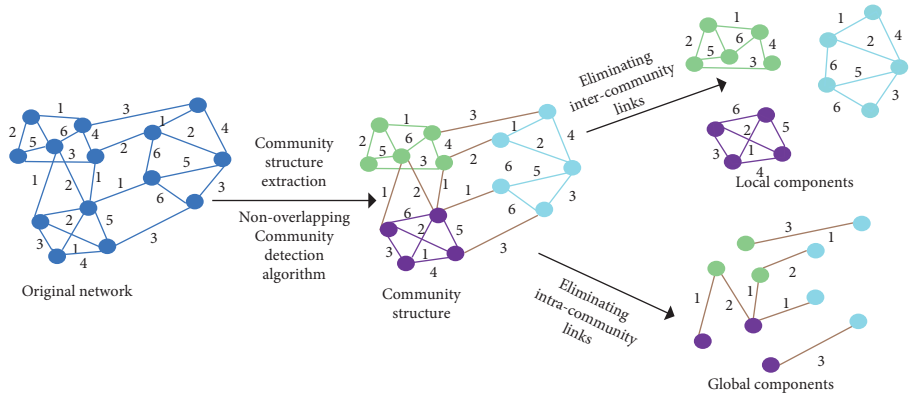


FIGURE 1: This figure illustrates the process of uncovering the component structure using a community detection algorithm to extract the dense parts forming the local components. After revealing the local components, one builds the global components with the nodes and links shared by the local components. In this example, the network has three communities colored green, light blue, and dark blue. Therefore, it has three local components. The links and nodes joining these local components form three global components.

surround cores. The component structure is an alternative mesoscopic representation. It states that a network consists of local and global components. Local components are the dense parts. The global components regroup the nodes and links connecting the local components. Uncovering the component structure proceeds as follows:

(1) Extract the dense parts of the network

(2) Eliminate the links between the dense parts to extract the local components

(3) Eliminate the links within the local components and the subsequently isolated nodes to extract the global components

Figure 1 illustrates the extraction process of the component structure. In this example, one uses a weighted nonoverlapping community detection algorithm to uncover the dense parts of the network. Then, we form the local components by removing the intercommunity links. Removing the intracommunity links and the isolated nodes extracts the global components. One can see that this representation is redundant. Indeed, a node can simultaneously belong to a local and a global component. However, it disentangles the local interactions from the global interactions.

2.2. Targeted Attack. One can consider two types of attacks in a network: random and targeted attacks. A random attack removes nodes randomly. It allows for studying the robustness of the network when an unexpected failure occurs. In contrast, targeted attacks aim to remove the most vital nodes for network connectivity [20, 21]. Centrality measures generally describe the importance of nodes [22–27]. In a strong attack strategy, one removes nodes in the network in the descending order of magnitude of a centrality measure. Weak attacks use the reverse order. This work evaluates the impact of strong attacks based on influential centrality measures for weighted networks: strength, betweenness, and PageRank.

2.3. Weighted Strength Centrality. A node's strength centrality [22] is the sum of the weights of its first-order neighbors. Given a graph G (V, E, and W), such as V is the number of nodes, E is the number of links, and W is the set of weights, the strength si of node i is defined as follows:

$$S_i = \sum_{j \in v, i=j} w_{ij}, \tag{1}$$

w_{ij} is an element of the adjacency matrix of G such as $w_{ij} = \alpha$ if i and j are connected, otherwise, wij = 0, $\alpha \in R_+^*$.

2.4. Weighted Betweenness Centrality. The betweenness [28] $b(i)$ of a node i is the fraction of the shortest path passing through it. When it is normalized, the betweenness of node i is defined as follows:

$$b(i) = \frac{2}{(n-1)(n-2)} \sum_{i=j}^{\sigma^w} \frac{j_k(i)}{\sigma_{j_k}^w}, \tag{2}$$

$\sigma_{j_k}^w$ is the number of the shortest path between j and k. $\sigma_{\mathrm{jk}}(\mathrm{i})^{\mathrm{w}}$ is the number of the shortest path from j to k passing in i.

2.5. Weighted PageRank Centrality. Initially introduced to rank websites, PageRank [29] is an iterative refinement measure based on a random walk process. Although defined for directed networks, one can use two directed links for undirected networks. For weighted network, it is defined as follows:

$$wpr_i(t) = \sum_{j=1}^{n} w_{ij} \frac{wpr_i(t-1)}{S_j^{\mathrm{out}}}, \tag{3}$$

S_j^{out} is the out-strength of node j.

3. Evaluation Measures

3.1. Largest Connected Component. The largest connected component (LCC) is the most popular metric to assess the robustness of a network [21, 30]. It refers to the largest connected component after removing a node and its links. Indeed, this operation can dislocate the network into several

Table 1: Basic topological properties of the world air transportation network, the five large local components, and the largest global component. N is the network size. $|E|$ is the number of edges. δ is the diameter. l is the average shortest path length. μ is the density. ζ is the transitivity, also called the global clustering coefficient. knn (k) is the assortativity, also called the degree correlation coefficient.

Components	N	$\|E\|$	δ	l	μ	ζ	knn(k)
World air transportation network	2734	16665	12	3,86	0,004	0,26	−0,05
North America-Caribbean	725	3794	7	3.14	0.014	0.28	−0.325
Europe-Russia	683	6016	6	2.85	0.025	0.32	−0.2
East and Southeast Asia-Oceania	630	3012	9	3.35	0.015	0.34	−0.22
Africa-Middle East-Southern Asia	313	989	7	3.37	0.02	0.28	−0.15
South America	201	494	6	3.2	0.024	0.23	−0.35
Large global component	557	2108	8	3	0.013	0.13	−0.25

independent components. It denotes the cohesiveness of the network and its ability to diffuse information. The higher the largest connected component, the most resilient the network is to the attack.

3.2. Weighted Efficiency. The efficiency [31] evaluates the exchange of information between the nodes of a network. Zhou et al. introduce the weighted efficiency in [11] to consider the influence of the link weights. In contrast to the unweighted efficiency, the weighted efficiency can be greater than 1. It is defined as follows:

$$WE(G) = \frac{1}{N(N-1)} \sum_{i,j \in v} \frac{1}{\sum_{I \in L_{ij}} 1/w_I}, \quad (4)$$

L_{ij} is the set of links on the shortest path between i and j. W_l is the weight of link l.

To assess the robustness of a network, this measure is recalculated after a node is removed from the network.

3.3. Jaccard Index. A Jaccard index [32] is used to compare the similarity of two sets. It is defined as follows:

$$J(P,Q) = \frac{|P \cap Q|}{|P \cup Q|}. \quad (5)$$

In the case of identical sets, the Jaccard index equals 1. In the absence of a shared element between two sets, it equals zero.

4. Data and Methods

4.1. Data. We use a weighted and undirected network. It represents the flight information collected during six days from FlightAware [33] (between May 17, 2018, and May 22, 2018). Nodes represent airports, and link weights represent the number of direct flights between airports. Table 1 presents its basic topological properties. One can see that the global air network is sparse. It is disassortative. In other words, large-degree nodes tend to connect with low-degree nodes. It has a large diameter. Indeed, one needs 12 flights to reach the most distant airports. The transitivity indicates that there are not many triplets. Consequently, rerouting is uneasy.

4.2. Methods. We extract the component structure of the world transportation network to evaluate the impact of a targeted attack on its regional and interregional constituents. The robustness evaluation process proceeds as follows:

(1) Disconnect a node from the world air transportation network according to an attack strategy
(2) Disconnect the same node from its local component
(3) Disconnect the same node from the global component if possible
(4) Extract the largest connected component from the world air transportation network
(5) Extract the largest connected component of the local components
(6) Extract the largest connected component of the global component.

This approach allows us to evaluate the impact of removing a critical airport in the world air transportation network on the regional and interregional networks. Figure 2 presents a toy example illustrating an attack on an airport of the world network and the effect on its components.

5. Component Structure

We use the weighted Louvain community detection algorithm [34, 35] to extract the dense parts of the network. It uncovers 17 communities. Therefore, there are 17 local components. Among them, there are five large components covering the following regions: (1) North America-Caribbean, (2) Europe-Russia, (3) East and Southeast Asia-Oceania, (4) Africa-Middle East- Southern Asia, and (5) South America. There are eight global components. The largest one includes more than 95% of the airports distributed worldwide [13]. Figure 3 represents the airports included in the large local and global components. We restrict our attention to these components in the robustness analysis.

Table 1 reports their basic topological properties. The diameter of the components quantifies the maximum number of links between two destinations in the component. Its value is around six and seven, except for the East and Southeast Asia-Oceania component, which requires a maximum of nine jumps to join two destinations. The global component's diameter is eight. It suggests that interregional relations are not very different from regional ones. The average path length confirms these results. On average, the Europe-Russia component requires less than three hops to

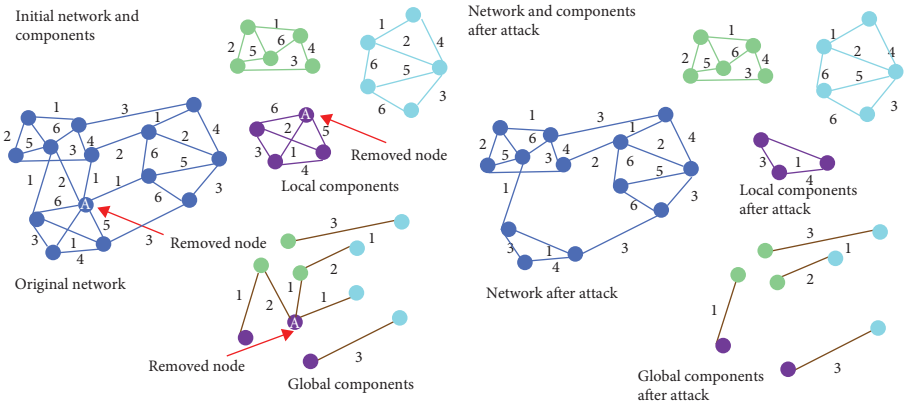


FIGURE 2: This toy example illustrates the influence of an attack on the network component structure. Removing node A in the original network impacts the dark blue local component (one node and three links are removed). It also affects the largest global component, which splits into two components with two nodes and an isolated node. Indeed, A has a global and local role.

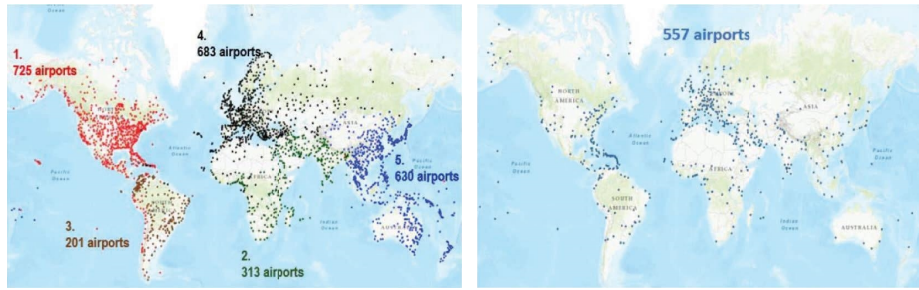


FIGURE 3: The figure at the left represents the airports in the uncovered large local components. They are in well-delimited geographic areas. Each color represents a component. (1) North America-Caribbean, (2) Europe-Russia, (3) East and Southeast Asia-Oceania, (4) Africa-Middle East-Southern Asia, and (5) South America. The figure at the right represents the airports of the largest global component. In contrast to local components, they are scattered all over the world.

travel between two airports. It takes more than three hops on average for all the other local components. With an average value of 3 for the large local component, interregional travels appear well organized compared to regional trips. Concerning the density of the components, one can distinguish two categories. The first class regroups the densest components: Europe-Russia, Africa-Middle East-Southern Asia, and South America. Indeed, their density is around 0.2. The second category contains North America-Caribbean, East and Southeast Asia-Oceania, and the large global component with a much lower density (about 0.13). With a transitivity value of 0.3, Europe-Russia and East and Southeast Asia components contain more interconnected triplets than the other components. Therefore, rerouting is more straightforward in these components. Note that the global component is less transitive. Assortativity measures the ability to connect nodes sharing similar degrees. All the components present various levels of disassortativity. In other words, airports with a high degree tend to connect with low-degree ones. The North America-Caribbean and the South America components are the most disassortative. This behavior is in line with the hub-and-spoke organizational model used in the airline industry. The Africa- Middle East-Southern Asia component is the less disassortative one.

6. Strength Targeted Attack

6.1. Evolution of the Largest Connected Component. Figure 4(a) gives the LCC as a function of the fraction of top strength nodes removed from the world air transportation network. It also reports the corresponding LCC values of the large components. All the curves reflect a similar behavior. As the fraction of top strength nodes increases, the size of the various LCC decreases almost linearly. The LCC of the Europe-Russia component decreases very slowly. Consequently, it is the most resilient region. The East-Southeast Asia-Oceania region follows. The Africa-Middle East-Southern Asia component is slightly below. One can distinguish two cases for the global component. Its size varies in high proportions below a threshold of around 8% of removed nodes. In contrast, above this threshold, it resists better to attacks and tends to be as resilient as the Europe-Russia component. The North America-Caribbean component is the most sensitive to the attack. The South American component behaves slightly better. Note that the LCC of the East-Southeast Asia-Oceania and North America-Caribbean components breaks down to around 20% when around 9% of their top airports are removed. One can observe that the size of the LLC of South America and

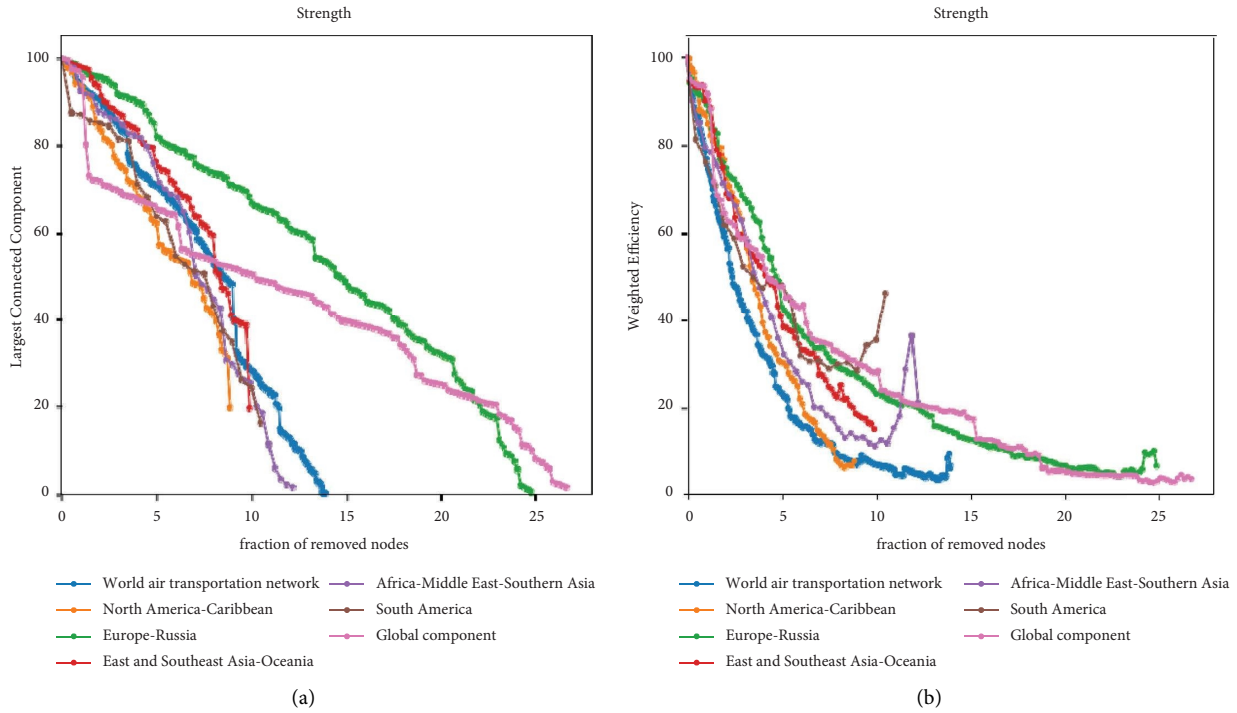


Figure 4: The figure at the left represents the fraction of nodes in the LCC of the large local and global components as a function of the fraction of removed nodes under a strength attack on the world air transportation network. We also represent the LCC of the world air transportation network in this situation. The Europe-Russia component and the global component are less sensitive to the attack. The figure at the right shows the weighted efficiency of the large local and global components as a function of the fraction of removed nodes under a strength attack on the world air transportation network. We also represent the weighted efficiency of the world air transportation network in this situation. Efficiency decreases at a high rate as the fraction of top strength nodes removed increases. Furthermore, the North America-Caribbean and Africa-Middle East-Southern Asia components appear to be the most vulnerable.

Table 2: Basic topological properties of the five local components isolated by the strength attack. λ is the size of the isolated component. ρ is the fraction of top strength nodes removed from the world air transportation network to isolate the component. δ is the diameter. l is the average shortest path length. μ is the density.

Components	ρ (%)	λ (%)	δ	l	μ
North America-Caribbean	9	19.86	14	5.7	0.021
Europe-Russia	13.5	21.5	18	7.96	0.019
East and Southeast Asia-Oceania	9.2	19.6	16	4.84	0.04
Africa-Middle East-Southern Asia	13.5	16.61	4	2	0,4
South America	11.4	16.4	7	3.69	0.063

the Africa-Middle East-Southern Asia components decreases similarly. Isolating a single node produces an abrupt reduction of the LCC. Indeed, removing a node separates an entire subnetwork from the component in this situation. For the other components and the world air transportation network, the variations of the LCC are more regular. The Europe-Russia component is a good illustration of this behavior. Indeed, it is almost a straight line. Nevertheless, removing a single node can also cause considerable damage to these networks. The world air transportation network is a typical example of brutal variations followed by quasilinear behavior.

As the fraction of removed nodes increases, the components break away from the world air transportation network one after the other. Table 2 displays information about the local components. We specify the fraction of nodes needed to isolate it from the world air transportation network. It also reports their giant component's size and basic topological properties after isolation.

North America-Caribbean is the first region isolated after removing 9% of the top strength airports of the overall network. Indeed, this component contains several airports with high traffic in the world. That is why, it is heavily targeted. The top 9% of airports include 9.1% of the airports of this component. Removing Piarco Airport in Trinidad and Tobago provoked the disconnection. The remaining airports form a network that contains 19.86% of the airport from the initial component. These airports are in the United States and Canada. The Alaska subregion is also isolated from the LCC. One can see that the diameter and the shortest path values double. Therefore, even though the LCC is denser than the initial component, it is more challenging to travel in the LCC.

East-Southeast-Asia-Oceania is the next separated component after disconnecting 9.2% of the top strength airports from the world air transportation. A proportion of 10% of the top airports belongs to this component. Beijing Nanyuan Airport in China was the last airport removed before isolation. The LCC includes 19.6% of the airports of the initial component, mainly in the Oceania area. Note that this component is cut in two. Indeed, the Beijing Nanyuan Airport is the last interaction between East-Southeast-Asia

and Oceania. Traveling within this LCC is more complicated than the initial component. Indeed, although denser than the original component, its diameter almost doubled, and the average shortest path increases by one hop.

Eliminating 11.4% of airports with the highest strength of the world air transportation network isolates South America. There are 11.4% of the airports belonging to this component among these airports. The separation occurs when removing Ministro Pistarini Airport in Argentina. Its LCC contains 16.4% of the airports of the initial component situated in Brazil and Venezuela. Traveling in the LCC is almost as easy compared to the initial component. Indeed, the diameter increases only by one. On average, it requires the same number of hops. In addition, the LCC is denser than the initial component.

Africa-Middle East-Southern Asia is the next region detaching from the world air transportation network. It happens after removing 13.5% of the top airports in the world. Among them, 17.8% of the airports belong to this component. India's Sardar Vallabhbhai Patel Airport is the last airport connecting it to the world. Once separated, the LCC of this component includes five airports distributed across five countries (Nepal, Bhutan, the United Arab Emirates, India, and Bangladesh). Except for the United Arab Emirates, these countries are neighbors.

Once these four components are separated, the European-Russia component remains the only component in the world air transportation network. It contains 21.5% of the airports of the initial component. They are in various countries. However, countries such as Portugal, Norway, Sweden, Turkey, and Spain are almost unreachable. In addition, except for Tajikistan, Central Asia and Transcaucasia countries are disconnected. The airports of Russia and Europe are still interconnected. Nevertheless, it is not easy to travel within this LCC. Indeed, the density is low, and the diameter and average shortest path are three times higher.

6.2. Weighted Efficiency. Figure 4(b) illustrates the evolution of the normalized weighted efficiency for the components and the world air transportation network under targeted strength attack. For the components, the curves report their values until they are isolated. Indeed, after isolation, their weighted efficiency does not change anymore. Indeed, removing a node in the world air transportation network does not affect the isolated component topology. One can observe a similar behavior on all the curves. Efficiency decreases at a high rate as the fraction of top strength nodes removed increases. One can notice a slightly different behavior for the Africa-Middle East-Southern Asia and the South America components. Before their isolation, the efficiency of these components increases. It is because airports located in a few countries compose their LCC. Overall, the European-Russia and the global components are less sensitive to strength targeted attacks in terms of efficiency. Conversely, the North America-Caribbean and Africa-Middle East-Southern Asia components appear most vulnerable. Let us now compare the component efficiencies after isolation from the world transportation networks.

Table 3: Evolution of the weighted efficiency and the LCC of the large local components after their isolation due to attacks based on strength. The order of isolation of the components is also presented. ωi is the weighted efficiency before attacks based on strength. ω is the weighted efficiency after the separation. λ is the largest connected component size after the separation. ρ is the fraction of top strength nodes removed from the world air transportation network to isolate the component. γ is the order in which the components are isolated. After their isolation, the components lose much of their efficiency.

Components	ω_i	ω	ω/ω_i (%)	λ (%)	ρ (%)	γ
North America-Caribbean	57.42	4	7	19.86	9	1
Europe-Russia	26.4	1.52	5.75	17.8	13.3	4
East and Southeast Asia-Oceania	31.31	4.85	15.4	19.6	9.6	2
Africa-Middle East-India	18.5	3.97	21.45	16.61	13.3	4
South America	23	10.7	46.5	16.4	11.4	3

Table 3 displays the initial value and the value after isolation of the weighted efficiency for the local components. One can see that the initial values are very different. Initially, the North America-Caribbean component is by far the most efficient. The East and Southeast Asia, Europe-Russia, and South America components follow. Finally, Africa-Middle East-Southern Asia is the less efficient local component.

After isolation, the South American local component is the most efficient. Indeed, few of its airports rank high in the world air transportation network. In addition, except for four airports in Venezuela, it includes only Brazilian airports. The Africa-Middle East-Southern Asia is the following component with the most significant efficiency. It contains only six airports located in different countries after isolation. East and Southern Asia-Oceania is next. It contains only airports from Oceania, located in several countries. Here again, an attack on the global air network has few consequences on regional traffic in Oceania. North America-Caribbean and the Europe-Russia components are the less efficient. Indeed, they include the top-rank hubs in the world air transportation network. Consequently, they lose numerous hubs. Note that the North America-Caribbean component is more efficient than Europe- Russia. Indeed, it includes several airports, but they are in only two countries. In contrast, airports are located in several European countries and Russia in the European-Russia component. One can notice that there seems to be no relationship between the order of isolation of the components and their relative efficiency after an attack.

7. Weighted Betweenness Targeted Attack

7.1. Evolution of the Largest Connected Component. Figure 5(a) reports the variation of the LLC while removing top betweenness centrality airports from the world air transportation network. One also plots the corresponding evolutions of the LCC for the components. The curves overlap until the fraction of the top nodes removed reaches around 2%. Beyond this value, they diverge.

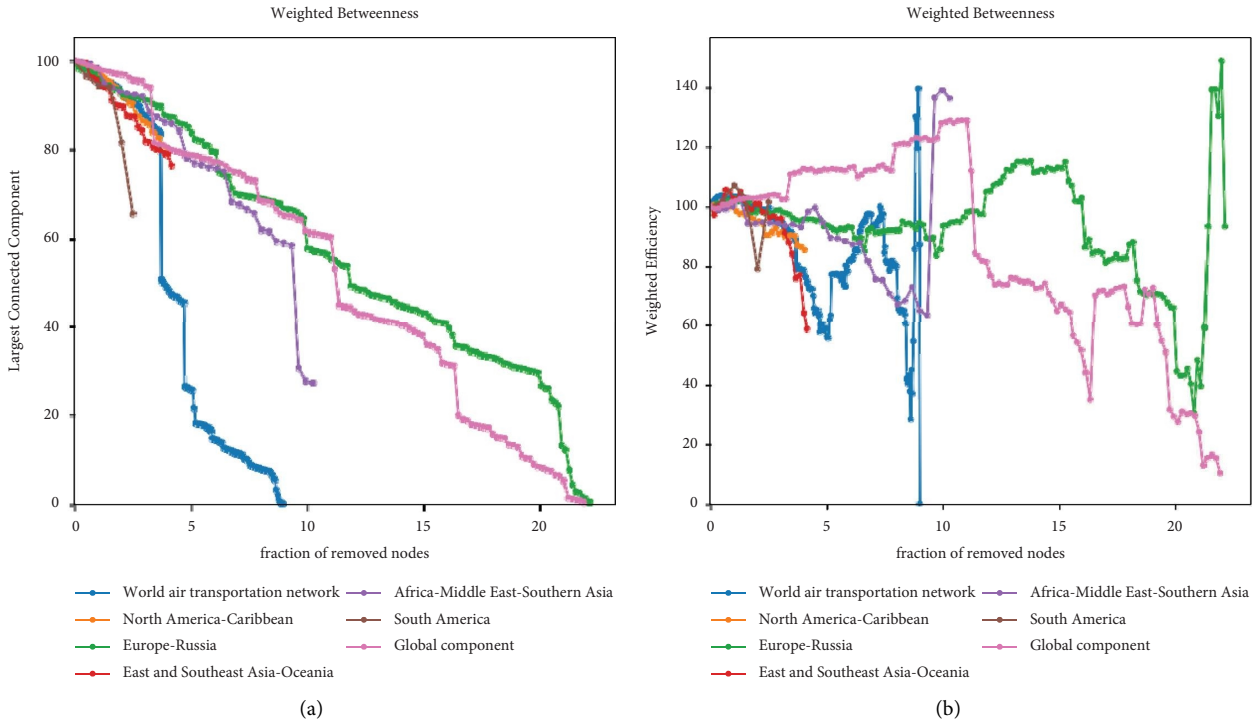


Figure 5: The figure at the left represents the fraction of nodes in the LCC of the large local and global components as a function of the fraction of removed nodes under a weighted betweenness attack on the world air transportation network. We also represent the LCC of the world air transportation network in this situation. The Europe-Russia component and the global component are less sensitive to the attack. The figure at the right shows the weighted efficiency of the large local and global components as a function of the fraction of removed nodes under a strength attack on the world air transportation network. We also represent the weighted efficiency of the world air transportation network in this situation. The weighted efficiency of the world air transportation network and the large components are very sensitive to attacks based on the betweenness centrality.

Table 4: Basic topological properties of the five local components isolated by the betweenness attack. λ is the largest connected component size. ρ is the fraction of top strength nodes removed from the world air transportation network to isolate the component. δ is the diameter. l is the average shortest path length. μ is the density.

Components	ρ (%)	λ (%)	δ	l	μ
North America-Caribbean	4.1	80	12	3.75	0.01
Europe-Russia	5.1	70	7	3.1	0.028
East and Southeast Asia-Oceania	4.7	76.5	17	4.77	0.012
Africa-Middle East-Southern Asia	5.1	27.4	6	3.28	0.045
South America	3.4	66.6	10	3.32	0.036

One can see that South America is the less resilient component, followed by the East and Southeast Asia-Oceania, the North America-Caribbean, and the Africa-Middle East-Southern Asia components. Europe-Russia and the global components exhibit similar behavior. Above 12% of removed airports, Europe-Russia takes the lead and becomes more resilient. One can see that the size of the LCC of North America-Caribbean, Europe-Russia, and the East-Southeast Asia-Oceania components decreases slowly. Piecewise linear variation with sharp drops characterizes the others, particularly the world air transportation network. Indeed, removing an airport can provoke significant damage. Table 4 reports the topological properties of the components once they are isolated from the network.

After removing 3.4% of the top betweenness airports from the world air transportation network, South America is the first isolated component. The attack contains only five airports (2.5%) of this component. They are in Venezuela, Brazil, Cuba, Colombia, and Argentina. Ministro Pistarini Airport in Argentina is the last liaison to the world. The LCC includes 65.6% of the airports of the initial component, distributed between all countries. The diameter and the density of the LCC are higher than in the initial component. In contrast, the average shortest path is comparable. Therefore, traveling within the LCC is almost as easy as traveling in the original component (Table 4).

The North America-Caribbean component is the second region that becomes unreachable after removing 3.7% of the top central airports of the world air transportation network. Among the 3.7% of top world airports, 4.1% belong to this component. The last airport connected to the other region is Orlando Airport in the United States. The LCC contains 80% of the airport of the initial component. These airports are scattered across all the countries. Even though the diameter is almost twice higher, it is always easy to travel between the remaining airports. Indeed, the average shortest path and the density increase slightly.

Table 5: Evolution of the weighted efficiency and the LCC of the large local components after their isolation due to attacks based on weighted betweenness. We also report the order of isolation of the components. ωi is the weighted efficiency before the attack based on weighted betweenness. ω is the weighted efficiency after the separation. λ is the largest connected component size after the split. ρ is the fraction of top weighted betweenness nodes removed from the world air transportation network to isolate the component. γ is the order in which the components are isolated. Globally, after their isolation, the efficiency of the LCC does not change much. Some LCCs are even more efficient.

Components	ω_i	ω	ω/ω_i (%)	λ (%)	ρ (%)	γ
North America-Caribbean	57.42	49.17	85.63	80	4.1	2
Europe-Russia	26.4	24.13	91.4	70	5.1	4
East and Southeast Asia-Oceania	31.31	18.4	58.76	76.5	4.7	3
Africa-Middle East-India	18.5	25.19	136.16	27.4	5.1	4
South America	23	23.37	101.6	66.6	3.4	1

Removing 4.7% of the top central airports of the world air network isolates the East and Southeast Asia region. The attack targets 4.1% of the airports of this component. Tokyo Haneda Airport in Japan is the last link to the world before the isolation. The size of the LCC decreases to 76.5% of the original component. Its airports are scattered across all the countries of the component. Nevertheless, air travel is more uneasy. Indeed, the LCC is less dense, and its diameter and average shortest path increase compared to the initial component.

Africa-Middle East-Southern Asia is the next isolated area. One needs to remove 5.1% of the top betweenness airport of the world air transportation network. There are 10.2% of the airports of this component among the top 5.1% of airports. Disconnecting the Borg El Arab Airport in Egypt isolates this region. 27.4% of the airports of the original component remain on the LCC. These airports are located only in the Middle East, Southern Asia, and Seychelles. Nevertheless, the United Arab Emirates, Yemen, and Oman are unreachable. Air travel in the LCC is more straightforward than in the initial component. Indeed, the diameter, the average shortest path, and the density are smaller.

Finally, only the Europe-Russia component remains on the world air transportation network. It includes 70% of airports of the initial component. All the countries of this component are well represented. Joining two airports of the LCC is slightly more complicated. Indeed, the diameter and the average shortest path increase. Note that the density also increases.

7.2. Weighted Efficiency. The weighted efficiency of the world air transportation network and the large components are very sensitive to the attacks based on the betweenness centrality, as shown in Figure 5(b). One can distinguish three typical behavior patterns for the efficiency variation versus the fraction of removed nodes. The first category includes the North America-Caribbean and East and Southeast Asia components. Their relative efficiency decreases almost monotonically as the fraction of removed nodes increases. This behavior is similar to the strength attack. Nevertheless, the efficiency of these components after the weighted betweenness attack is less impacted. The second category concerns the Africa-Middle East-Southern Asia and South America components. In this case, the efficiency decreases as in the first category. However, before the component splits from the network, its efficiency increases. The third category regroups the European-Russia component, the global component, and the world air transportation network. Large variations of efficiency characterize it. Indeed, the weighted betweenness attack isolates the peripheral subregions successively so that the weighted efficiency can surpass its initial value.

Table 5 displays the initial value of the weighted efficiency for the local components and the value after their isolation. After isolation, the Africa-Middle East-Southern Asia component is much more efficient. Indeed, while it initially covers many countries, the isolated component exclusively contains airports in the Middle East and Southern Asia (except for two airports in Seychelles). As these two regions are very well connected, the component efficiency increases even though it loses numerous hubs.

The South American component efficiency increases slightly compared to its initial value. Indeed, most of the removed airports by the attack are in Brazil. Overall, other countries still have essential airports to maintain travel efficiency. The North America-Caribbean component is the second isolated component. It loses 15% of its efficiency while preserving 80% of its airports. The United States and Canadian airports are the most vulnerable to the attack. Nevertheless, some essential airports in different countries remain in this component. Travel becomes more challenging but well guaranteed.

The European-Russia component is the next most efficient. Despite being heavily attacked, this component loses less than 10% of its efficiency while keeping 70% of its initial nodes. As the isolated part preserves several hubs in Europe, traffic within European airports is still efficient. However, reaching and traveling in Russian area is more complicated. Indeed, air transport in Russia depends on a few hubs. Once attacked, traveling in and to the region becomes more challenging.

The East-Southeast-Asia-Oceania component is more impacted by the attack. It loses more than 40% of its efficiency while keeping more than 70% of its airports. Indeed, a strong hub and spoke topology characterizes this region. The attack removes important hubs in China and Oceania involved in the traffic between these two regions. Consequently, the global efficiency of the component decreases drastically.

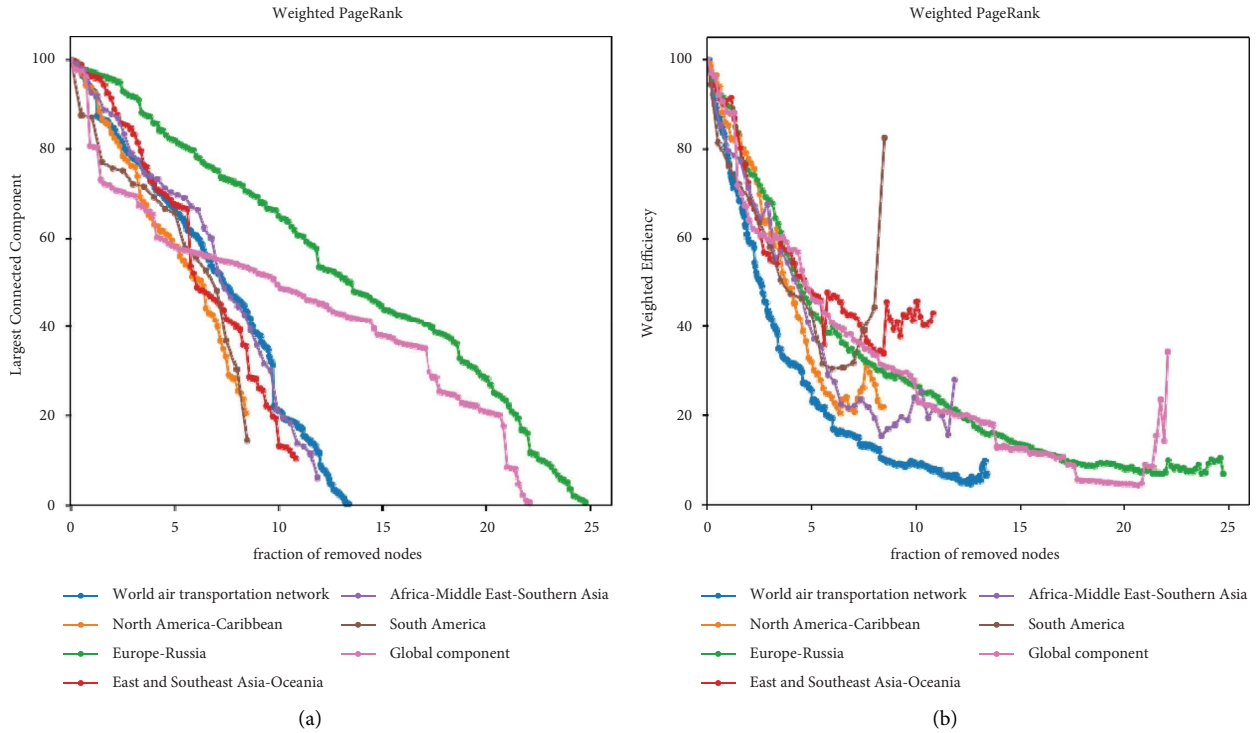


Figure 6: The figure at the left represents the fraction of nodes in the LCC of the large local and global components as a function of the fraction of removed nodes under a weighted PageRank attack on the world air transportation network. We also represent the LCC of the world air transportation network in this situation. The Europe-Russia component and the global component are less sensitive to the attack. The figure at the right shows the weighted efficiency of the large local and global components as a function of the fraction of removed nodes under a strength attack on the world air transportation network. We also represent the weighted efficiency of the world air transportation network in this situation. The world air transportation network appears as the most vulnerable.

8. Weighted PageRank Targeted Attack

8.1. Evolution of the Largest Connected Component. Figure 6(a) presents the variation of the LCC for the five local components and the world air transportation network when removing the top weighted PageRank nodes in the world air transportation network. One can see that the European-Russia component is the most resilient. Indeed, its curve is above all the others, whatever the fraction of removed nodes. The other local components exhibit similar behavior. Their sizes decrease almost linearly in equal proportions. Nevertheless, one can notice that globally, the North America-Caribbean and South American components are the most sensitive to the weighted PageRank attacks. For the global component, we can distinguish two situations. It behaves like the mainstream local components until it reaches a fraction of 7% removal of the top-weighted PageRank airports. Above this value, it tends to follow the European-Russia component.

Removing 8.11% of the top-ranked airports in the world air transportation network isolates the North America-Caribbean component. The attack concerns only 8.4% of the airports in this component. Southwest Florida Airport in the United States was the last airport allowed to reach the rest of the world. Its LCC includes 20.4% of the airports of the initial component. They cover the initial component area, except for Alaska, Chile, and a large part of Canada.

Table 6: Basic topological properties of the local components isolated by the weighted PageRank attack. λ is the largest connected component size. ρ is the fraction of top strength nodes removed from the world air transportation network to isolate the component. δ is the diameter. l is the average shortest path length. μ is the density.

Components	ρ (%)	λ (%)	δ	l	μ
North America-Caribbean	8.1	20.4	17	6.11	0.021
Europe-Russia	13.2	16.7	13	6.10	0.022
East and Southeast Asia-Oceania	12	10.47	8	3.82	0.045
Africa-Middle East-Southern Asia	13.2	6	8	4	0.13
South America	9.7	14.9	6	3	0.09

Comparing its topological properties with the initial component, one can say that it is more difficult to travel in the isolated component. Indeed, as shown in Table 6, even though the density increases, the diameter and the average shortest path values are two times higher.

South America separates next from the world air network after removing 9.7% of airports. Among these airports, only 8.4% belong to this component. Simon Bolivar Airport in Venezuela is the last airport connected to the world. Once isolated, 14.9% of the airports in the initial component remain in this LCC. Except for four airports in Venezuela, they are all in Brazil. Note that the topological properties of

Table 7: Evolution of the weighted efficiency and the LCC of the large local components after their isolation due to attacks based on weighted PageRank. We also report the order of isolation of the components. ωi is the weighted efficiency before the attack based on PageRank. ω is the weighted efficiency after the separation. λ is the largest connected component size after the split. ρ is the fraction of top PageRank nodes removed from the world air transportation network to isolate the component. γ is the order in which the components are isolated. Isolating the components reduces their efficiency significantly.

Components	ω_i	ω	ω/ω_i (%)	λ (%)	ρ (%)	γ
North America-Caribbean	57.42	12.55	21.85	20.4	8.4	1
Europe-Russia	26.4	1.86	7	17.8	13.4	4
East and Southeast Asia-Oceania	31.31	13.51	43.14	10.47	12	3
Africa-Middle East-India	18.5	5.19	28	6	13.4	4
South America	23	18.95	82.4	14.4	9.7	2

Table 8: This table summarizes the results for the attacks under evaluation (strength, weighted betweenness, and weighted PageRank). We report the order of isolation, the proportion of airports removed, and the LCC of the local component. The Jaccard index between LCCs for attack pairs is reported for each large component. γs, γb, and γp are, respectively, the order of isolation of the LCC from strength, weighted betweenness, and weighted PageRank. ρs, ρb, and ρp are, respectively, the proportion of attacked airports from the world air transportation network according to the strength, weighted betweenness, and weighted PageRank. λs, λb, and λp are, respectively, the LCC from strength, weighted betweenness, and weighted PageRank. Jsb, Jsp, and Jbp represent, respectively, the Jaccard index of the LCCs isolated by strength and weighted betweenness, strength and weighted PageRank, and weighted betweenness and weighted PageRank.

Components	γs	γb	γp	ρs(%)	Pb (%)	ρp(%)	λs(%)	λb(%)	λp(%)	Jsb	Jsp	Jbp
North America-Caribbean	1	2	1	9.1	4.1	8.1	19. 86	80	20.4	0.23	0.017	0.25
Europe-Russia	4	4	4	13.2	5.3	13.4	21.5	70	16.7	0.25	0.69	0.2
East and Southeast Asia-Oceania	2	3	3	9.2	4.7	12	19.6	76.5	10.47	0.2	0	0.13
Africa-Middle East-Southern Asia	4	4	4	13.2	5.3	13.4	16.61	27.4	6	0	0	0
South America	3	1	2	11.4	3.4	9.7	16.4	66.6	14.9	0.25	0.46	0.22

the LCC are similar to the initial component. Therefore, the regional traffic is not affected much.

Removing 12% of the airports from the global air network isolates the East and Southeast Asia-Oceania component. At this point, the attack concerns only 10.8% of the airports in this component. Lhasa Gonggar Airport in China was the last link to the rest of the world. The LCC reduces to 10.47% of the initial component size, with its airports scattered in nine countries. However, they are not well distributed. Indeed, there are no airports in Oceania, and half of them are in China airports. Although the component shrinks a lot, covering a more concentrated area makes travel more straightforward in what remains. Indeed, the airports of the LCC are well connected compared to the initial component.

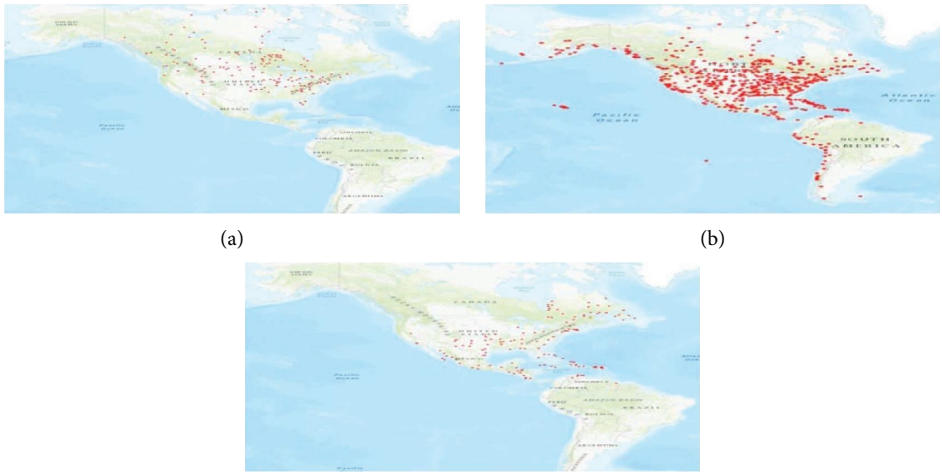
The Africa-Middle East-Southern Asia component disconnects from the whole network when the attack involves 13.2% of the top airports. Among these airports, only 12.21% belong to this component. Khartoum Airport in Sudan is the last link to the world. Only 6% of the airports remain connected in the LCC. They are in East Africa and islands such as Madagascar, La Reunion, and so on. However, the LCC covers a more compact and denser area than the initial component. In addition, the diameter increases by one hop, while the average shortest path does not change. Therefore, the local travel experience in the LCC is comparable to the initial component.

Once all the components are isolated from the world air network, only the Europe-Russia component remains. Moreover, the LCC connects 16.7% of the initial airports in this component. It includes airports from various countries except for Portugal, Finland, Kazakhstan, and Turkey, which have become unreachable. The diameter and the average shortest path length values are two times higher than in the initial component. In addition, the density decreases. Consequently, traveling in what remains of the component is much more difficult.

8.2. Weighted Efficiency. Figure 6(b) displays the variation of the weighted efficiency of the components and the world air transportation network when the top weighted PageRank airports are removed iteratively from the world air transportation network. The world air transportation network appears as the most vulnerable. Results for the components are more mixed. Until the attack involves 5% of the airports, curves are very close. After this threshold, Europe-Russia and the global component are the most efficient. Moreover, we distinguish two types of curves.

In the first type, we observe that the weighted efficiency increases before the isolation. It is the case of East and Southeast Asia-Oceania, Africa-Middle East-Southern Asia, South America, and the global components. Indeed, the attack splits the component into multiple subregions. Therefore, the airports in the LCC cover a small area facilitating the regional exchanges well, even though one cannot reach some top PageRank airports. The second type concerns the North America, Europe-Russia components. Indeed, these components lose several top PageRank airports, making regional travel more challenging.

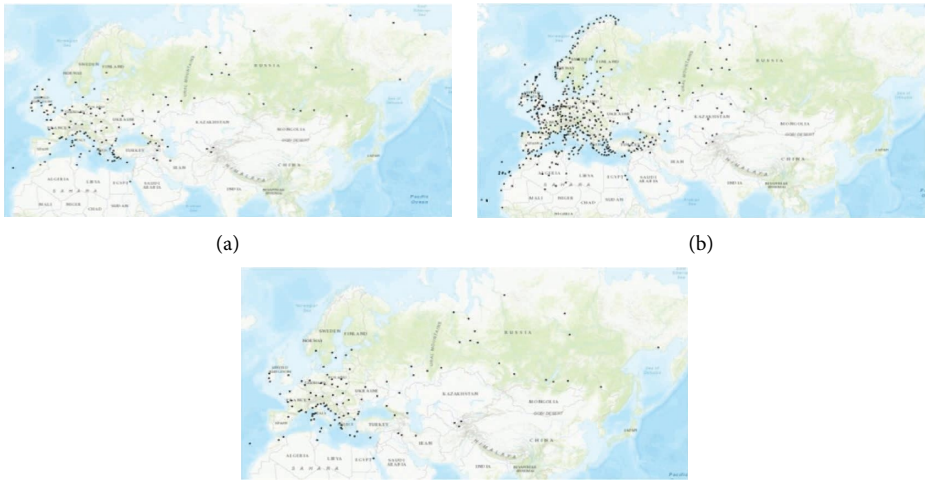
Table 7 presents the weighted efficiency of the components and the world air transportation network before the



(a) (b)

(c)

Figure 7: LCC of the North America-Caribbean component after its isolation from the network. The red dots are the remaining airports after attacks on the world air transportation network (a) strength attack, (b) weighted betweenness attack, and (c) weighted PageRank attack. The airports in the LCC isolated by the strength and weighted PageRank attacks are concentrated in the US and a small part of Canada. In contrast, airports are scattered in all the areas covered by the initial component after the weighted betweenness attack.



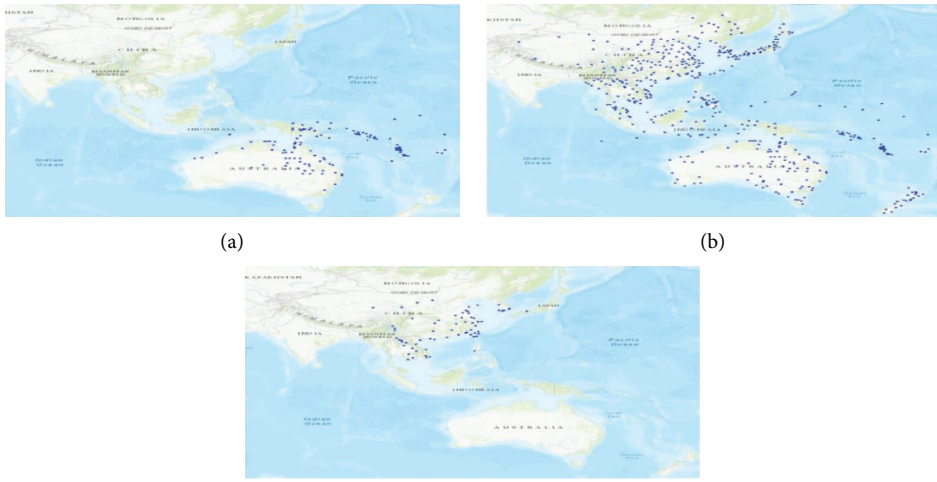
(a) (b)

(c)

Figure 8: LCC of the Europe-Russia component after its isolation from the network. The black dots are the remaining airports after attacks on the world air transportation network (a) strength attack, (b) weighted betweenness attack, and (c) weighted PageRank attack. The LCC isolated by the strength and weighted PageRank attacks covers almost all countries sparsely. The LCC is well distributed in all the initial component areas for the weighted betweenness attack.

attack and after the isolation of the LCC. In that case, the attack always translates into a lower efficiency. The South American component is the less vulnerable, with an efficiency decreasing by less than 20%. Indeed, the isolated component contains essentially Brazilian airports. Furthermore, it covers mainly the northern parts of Brazil, near Venezuela. This reduced coverage compared to the initial component makes it quite efficient.

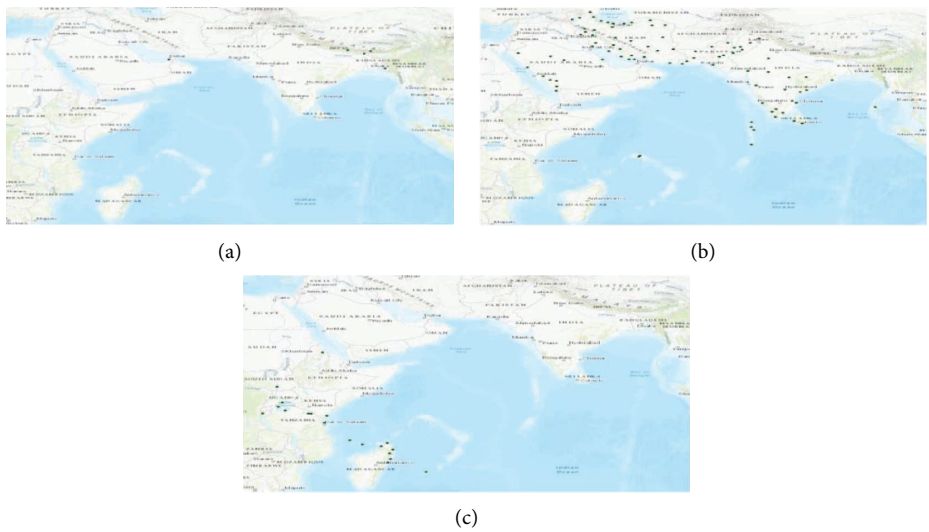
The East and Southeast Asia-Oceania component follows. Its efficiency after the attack drops to around 40% of its initial value. There are no airports from Oceania in the LCC. Most of them are in the East of China and its satellite countries. Therefore, the relative preservation of the efficiency also comes at the cost of a smaller geographical coverage. The Africa-Middle East-Southern Asia reduces its efficiency to 28% of its initial value. In this case also, the airports are concentrated in a reduced area. Indeed, the isolated component includes only airports in East Africa and Madagascar. The North America-Caribbean component is susceptible to the attack. Once isolated, its efficiency reduces by around 20% of its initial value. However, the isolated component by PageRank covers almost all the original regions. Europe-Russia is the most affected component by the weighted PageRank attack. It loses several hubs. In addition, many peripheral subregions, including secondary airports, remain in the isolated component. This is why, its weighted efficiency reduces to 7% of its initial value.



(a) (b)

(c)

Figure 9: LCC of the East and Southeast Asia-Oceania components after isolation from the network. The blue dots are the remaining airports after attacks on the world air transportation network (a) strength attack, (b) weighted betweenness attack, and (c) weighted PageRank attack. The LCC isolated by the strength attack covers the countries in Oceania. The LCC separated by the weighted PageRank attack covers East and Southeast Asia major countries. In contrast, the LCC isolated by the weighted betweenness attack covers all the regions of the initial component.



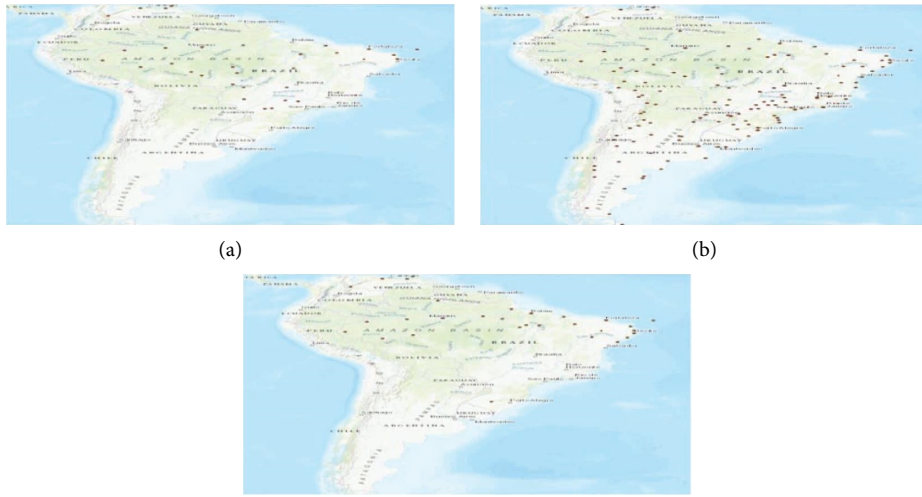
(a) (b)

(c)

Figure 10: LCC of the Africa-Middle East-Southern Asia component after isolation from the network. The green dots are the remaining airports after attacks on the world air transportation network (a) strength attack, (b) weighted betweenness attack, and (c) weighted PageRank attack. The LCC isolated by the strength attack covers five countries (Nepal, Bhutan, the United Arab Emirates, India, and Bangladesh). The LCC isolated by the weighted PageRank attack covers East Africa and Madagascar countries. The LCC separated by the weighted betweenness attack covers mainly the Middle East and Southern Asia countries.

9. Comparing the Attacks

9.1. Evolution of the Largest Connected Component. Table 8 displays the order of isolation of the local components for the various attacks. Although it changes with the attack, one can observe some trends. The North America-Caribbean region tends to leave first the world air transportation network. South America, which is very connected to the North America-Caribbean component, generally follows it. Indeed, once the North America-Caribbean component leaves the global air network, South America has fewer connections with the rest of the world. Furthermore, these connections are with the worldwide most important airports that are easily targeted. Then, the



(a) (b) (c)

Figure 11: LCC of the South America component after isolation from the network. The brown dots represent the remaining airports after attacks on the world air transportation network (a) strength attack, (b) weighted betweenness attack, and (c) weighted PageRank attack. The LCC isolated by the strength and weighted PageRank attacks includes Brazil and Venezuela. The LCC separated by the weighted betweenness attack covers all the initial component regions.

Table 9: Variation of the weighted efficiency of the different attacks once the component splits from the overall network. ωs, ωb, and ωp, are, respectively, the fraction of the weighted efficiency of the LCCs for strength, weighted betweenness, and weighted PageRank attacks. The weighted betweenness attack does not impact much the efficiency of the components compared to the other attacks.

Components	ω_s/ω_i (%)	ω_b/ω_i (%)	ω_p/ω_i (%)
North America-Caribbean	7	85.6	21.85
Europe-Russia	5	91.4	7
East and Southeast Asia-Oceania	15	58.7	43.14
Africa-Middle East-Southern Asia	21.45	113.6	28
South America	46.5	101	82.5

East-Southeast Asia-Oceania component gets isolated. Finally, the attack strategy separates Africa-Middle East-Southern Asia from the Europe-Russia component. Indeed, due to their geographic and political relations, these two components are inextricably linked.

Table 8 also reports the fraction of removed airports to isolate the components. The weighted betweenness attack is the most effective. Indeed, it needs to remove less than half as many airports compared to its alternatives to separate the components. Strength and PageRank need similar resources to reach the same goal.

Table 8 presents the fraction of airports in the LCC of the components after breaking away from the world transportation network. Globally, the weighted betweenness attack tends to maintain a large fraction of the airports included in the initial component (around 70%). It is not the case for the Africa-Middle East-Southern Asia component. Indeed, the last region to be isolated is divided into multiple subregions so that the LCC contains only 28% of the initial airports. Strength and PageRank seem comparable with a slight advantage to strength. They preserve, respectively, around 20% and 15% of the size of the initial components.

The Jaccard index between the couples of attacks reported in Table 8 shows that globally, the largest connected components have few airports in common. The highest score of 0.69 concerns the Europe-Russia component and the strength and PageRank attacks. The lowest score is zero. It concerns the three couples of attack for the Africa-Middle-East-Southern Asia component and PageRank and strength for the East and Southeast Asia components. In all these cases, the isolated components have no airport in common.

Figures 7–11 represent the airports in the LCC after the attack for the five local components. They demonstrate the lower regional impact of weighted betweenness on the isolated largest connected components. One can also note that except for the North America-Caribbean component, the isolated components by the weighted PageRank are smaller than the strength attack.

In addition, it shows that the isolated components in the same region do not cover the same areas. Indeed, although of similar size, the LCC of the weighted PageRank attack covers more than 20 countries. In contrast, the LCC derived from the strength attack covers only the United States and Canada. It confirms the low value of the Jaccard index coefficient. Indeed, the two LCCs have only five airports in common, and even airports in the same country are different.

The LCCs derived from the strength and PageRank attacks of the South America component are comparable in size. They cover Brazil and Venezuela. In Venezuela, they include the same four airports. With a Jaccard index near 0.5, the difference is in Brazil. Nevertheless, they have 10% of

the airports in common. The LCCs from the strength and weighted PageRank attacks of Europe-Russia cover the same geographical area. As reflected by the Jaccard index value (0.7), they have several airports in common (15.6%). The LCCs of the East and South East Asia-Oceania regions have no airports in common. Indeed, for the strength attack, the LCC includes only the airports in the Oceania component, whereas the PageRank attack includes airports in East and Southeast Asia. The same observation holds for the Africa-Middle-East-Southern Asia component. Indeed, the LCC of the strength attack is in Southern Asia, while it is in Africa for PageRank. To summarize, PageRank and strength attacks have a comparable impact on the robustness of the local components. However, qualitatively, they are very different. Indeed, the isolated components cover different regions.

The weighted betweenness attack isolates the components earlier compared to their alternatives. Consequently, the separated LCCs contain 2 to 3 times more airports covering larger geographical areas. Therefore, its Jaccard index with the other attacks is small. However, the largest isolated components by the strength attack share more than 80% of its airports with the weighted betweenness LCC in the North America-Caribbean, Europe-Russia, and East and Southeast Asia components. The PageRank LCCs share more than 90% of their airports with the weighted betweenness LCCs in these components. The LCC of the weighted be tweenness includes all the airports in the LCCs of the two other attacks in South America. In contrast, all the LCCs are disjoint in the Africa-Middle East-Southern Asia.

9.2. Weighted Efficiency. Table 9 displays the variation of the weighted efficiency of the local components subject to the different attacks. With an average weighted efficiency equal to 90% of its original value, the weighted betweenness attack is less disturbing for regional trips. Note that in the Africa-Middle-East-Southern Asia and South America components, it is more efficient to travel in the separated components than in its initial version. Indeed, they are more compact. The PageRank attack is more disturbing, with an average of 36% compared to the initial values. Strength is the most disruptive attack. Indeed, the average efficiency fraction drops to 18%. Going into more detail, we observe that the LCC of the South America component keeps a high weighted efficiency regardless of the attack. Its value ranges from 46.5% to 82.5%. As the LCCs include mainly airports in Brazil and Venezuela, traveling in what remains from the original component is still manageable. We observe similar behavior for the Africa-Middle East-Southern Asia component. Its weighted efficiency ranges from 21.45% to 131.6%. In any case, the LCCs of this component correspond to different well-interconnected subregions. The East and Southeast Asia-Oceania preserve a relatively good efficiency, notably for the betweenness and PageRank attacks. The LCC is in Oceania for the strength attack and the East and Southeast Asia subregion for the PageRank attack. The North America-Caribbean region exhibits a low-efficiency after a strength attack. Despite its LCC covering only two countries, its efficiency is low because it loses several hubs. It is three times more efficient after a PageRank attack. Indeed, the LCC covers several countries while maintaining more hubs. Thus, the regional traffic is less degraded. Europe-Russia has the lowest efficiency for strength and PageRank attacks. This component loses several hubs in Europe and Russia despite covering all countries. Thus, traffic between the European and Russian regions becomes very challenging. Overall, one can say that the more reduced area the LCC of the components covers, the more efficient they are, except for when the attack targets many hubs, such as North America-Caribbean and Europe-Russia components.

10. Conclusion

The component structure represents the air transportation network as an aggregate of interconnected regional networks. It allows for investigating the impact of targeted attacks on the air transport network on its regional and interregional constituents. This study investigates the strength, weighted betweenness, and weighted PageRank attacks on networks weighted by the number of flights.

In the three attack strategies, the different areas break away successively when removing a given fraction of critical airports from the world air transportation network. Nevertheless, the order of isolation of the regions differs. After the strength attack, North America-Caribbean, East-Southeast Asia-Oceania, and South America leave the world air transportation network. South America, North America-Caribbean, and the East and Southeast Asia-Oceania regions disconnect in this order after removing top weighted betweenness airports from the world air network. Attacking the top weighted PageRank airports isolates in sequence North America-Caribbean, South America, East, and Southeast Asia-Oceania. Finally, in any case, Africa-Middle East-Southern Asia and Europe-Russia are the last to split.

The weighted world air transportation network is more vulnerable to weighted betweenness attacks than its alternatives under test. Indeed, one needs to remove fewer vital airports in the weighted betweenness attack to isolate the different regions. Nevertheless, in this case, the LCCs of the isolated components contain a high fraction of the initial component structure. It allows them to keep and even improve their regional efficiency. The LCCs of the components obtained with a budget of removed airports in the same order of magnitude using the strength and PageRank attacks are much smaller. At first glance, they may seem comparable with a slight advantage for strength at preserving a higher fraction of the original component airports. However, their content is quite different. Most often, they cover different subregions.

The impact of the different attacks in terms of weighted efficiency in what remains of the five initial components is not uniform. Globally, weighted betweenness is the less disruptive, followed by PageRank and strength. The proportion of hubs involved in the attack, the order of separation of the components, and the geographical compactness of the LCC exert a significant influence on the local efficiency.

The component structure allows a better understanding of the resilience of the global air transportation network. The weighted betweenness attack rapidly dismantles the world air transportation network by isolating large geographic areas. However, this vulnerability is relative since travel in these areas remains seamless. Future work will focus on developing attack strategies tailored to the component structure. We also plan to perform a comparative analysis with the unweighted world air transportation network.

Data Availability

The weighted and undirected network that we use represents the flight information collected during six days from FlightAware\cite (FlightAware) (between May 17, 2018, and May 22, 2018). Nodes represent airports, and link weights represent the number of direct flights between airports. The data are already used in (https://doi.org/10.1088/1367-2630/ab687c). The (DATA TYPE) data used to support the findings of this study are available from the corresponding author upon request.

Conflicts of Interest

The authors declare that they have no conflicts of interest.

References

[1] M. Jusup, P. Holme, K. Kanazawa et al., "Social physics," *Physics Reports*, vol. 948, pp. 1–148, 2022.

[2] O. Lordan, J. M. Sallan, and P. Simo, "Study of the topology and robustness of airline route net- works from the complex network approach: a sur- vey and research agenda," *Journal of Transport Geography*, vol. 37, pp. 112–120, 2014.

[3] X. Sun and S. Wandelt, "Robustness of air transportation as complex networks: system- atic review of 15 years of research and outlook into the future," *Sustainability*, vol. 13, no. 11, p. 6446, 2021.

[4] J. T. Aparicio, E. Arsenio, and R. Henriques, "Assessing robustness in multimodal transportation systems: a case study in lisbon," *Eu- ropean Transport Research Review*, vol. 14, no. 1, pp. 28–18, 2022.

[5] Lu Zhang, H. Du, X. Zhang, P. De Maeyer, B. Dessein, and Y. Zhao, "Ro- bustness and edge addition strategy of air transport networks: a case study of "the belt and road"," *IEEE Access*, vol. 7, pp. 96470–96477, 2019.

[6] T. Verma, N. A. M. Araújo, and H. J. Herrmann, "Revealing the structure of the world airline network," *Scientific Reports*, vol. 4, no. 1, pp. 1–6, 2014.

[7] S. Wandelt, X. Shi, and X. Sun, "Estimation and improvement of transportation net- work robustness by exploiting communities," *Reliability Engineering & System Safety*, vol. 206, Article ID 107307, 2021.

[8] O. Lordan, J. M. Sallan, P. Simo, and D. Gonzalez-Prieto, "Robustness of the air transport network," *Transportation Research Part E: Logistics and Transportation Review*, vol. 68, pp. 155–163, 2014.

[9] X. Sun, V. Gollnick, and S. Wandelt, "Robustness analysis metrics for world- wide airport network: a comprehensive study," *Chinese Journal of Aeronautics*, vol. 30, no. 2, pp. 500–512, 2017.

[10] X. Bao, P. Ji, W. Lin, M. Perc, and J. . Kurths, "The impact of covid-19 on the worldwide air transportation network," *Royal Society Open Science*, vol. 8, no. 11, Article ID 210682, 2021.

[11] Y. Zhou, J. Wang, and G. Q. Huang, "Efficiency and robustness of weighted air transport networks," *Transportation Research Part E: Logistics and Transportation Review*, vol. 122, pp. 14–26, 2019.

[12] S. Kim and Y. Yoon, "On node criticality of the northeast asian air route network," *Journal of Air Transport Management*, vol. 80, Article ID 101693, 2019.

[13] I. M. Diop, C. Cherifi, C. Diallo, and H. Cherifi, "Revealing the component structure of the world air transportation network," *Applied Network Science*, vol. 6, no. 1, pp. 92–50, 2021.

[14] I. Moussa Diop, C. Cherifi, C. Diallo, and H. Cherifi, "Robustness of the weighted world air transportation network components," in *Proceedings of the 2022 IEEE Workshop on Complexity in Engineer- ing (COMPENG)*, pp. 1–6, Florence, Italy, July 2022.

[15] Di Jin, Z. Yu, P. Jiao et al., "A survey of community detection approackhes: from statistical modeling to deep learning," *IEEE Transactions on Knowledge and Data Engineering*, 2021.

[16] H. Cherifi, G. Palla, B. K. Szymanski, and X. Lu, "On community structure in complex networks: challenges and opportuni- ties," *Applied Network Science*, vol. 4, no. 1, pp. 117–135, 2019.

[17] K. Orman, L. Vincent, and H. Cherifi, "An empirical study of the relation between community structure and transitivity," in *Complex Networks*, pp. 99–110, Springer, Berlin, Heidelberg, 2013.

[18] W. Tang, L. Zhao, W. Liu, Y. Liu, and Bo Yan, "Recent advance on detecting core- periphery structure: a survey," *CCF Transac- tions on Pervasive Computing and Interaction*, vol. 1, no. 3, pp. 175–189, 2019.

[19] S. Kojaku and N. Masuda, "Finding multiple core-periphery pairs in networks," *Physical Review E - Statistical Physics, Plasmas, Fluids, and Related Interdisciplinary Topics*, vol. 96, no. 5, Article ID 052313, 2017.

[20] Z. Wan, Y. Mahajan, B. W. Kang, T. J. Moore, J. H. Cho, and J.-H. Cho, "A survey on cen- trality metrics and their network resilience analy- sis," *IEEE Access*, vol. 9, pp. 104773–104819, 2021.

[21] S. Wandelt, X. Sun, D. Feng, M. Zanin, and S. Havlin, "A comparative analysis of approaches to network- dismantling," *Scientific Reports*, vol. 8, no. 1, pp. 13513–13515, 2018.

[22] L. Lü, D. Chen, X.-L. Ren, Q.-M. Zhang, Yi-C. Zhang, and T. Zhou, "Vital nodes identification in complex net- works," *Physics Reports*, vol. 650, pp. 1–63, 2016.

[23] Z. Ghalmane, C. Cherifi, H. Cher- ifi, and M. E. Hassouni, "Centrality in complex networks with overlapping community structure," *Scientific Reports*, vol. 9, no. 1, ArticleID 10133, 29 pages, 2019.

[24] S. Rajeh, M. Savonnet, E. Leclercq, and H. Cherifi, "Interplay between hierarchy and centrality in complex networks," *IEEE Access*, vol. 8, pp. 129717–129742, 2020.

[25] D. Chakraborty, A. Singh, and H. Cherifi, "Immunization strategies based on the over- lapping nodes in networks with community struc- ture," in *International Conference on Computational Social Networks*, pp. 62–73, Springer, Berlin, Germany, 2016.

[26] M. Kumar, A. Singh, and H. Cher- ifi, "An efficient immunization strategy using over- lapping nodes and its neighborhoods," in *Proceedings of the Companion The Web Conference 2018*, pp. 1269–1275, Lyon, France, April 2018.

[27] A. Ibnoulouafi, M. El Haziti, and H. Cherifi, "M-centrality: identifying key nodes based on global position and local degree variation," *Journal of Statistical Mechanics: Theory and Experiment*, vol. 2018, no. 7, Article ID 073407, 2018.
[28] U. Brandes, "A faster algorithm for between- ness centrality," *Journal of Mathematical Sociology*, vol. 25, no. 2, pp. 163–177, 2001.
[29] Y. Ding, "Applying weighted pagerank to au- thor citation networks," *Journal of the American Society for Information Science and Technology*, vol. 62, no. 2, pp. 236–245, 2011.
[30] M. Oehlers and B. Fabian, "Graph metrics for network robustness—a survey," *Mathematics*, vol. 9, no. 8, p. 895, 2021.
[31] P. Crucitti, V. Latora, M. Marchiori, and A. Rapisarda, "Efficiency of scale-free net- works: error and attack tolerance," *Physica A: Statistical Mechanics and its Applications*, vol. 320, pp. 622–642, 2003.
[32] L. da F. Costa, "Further generalizations of the jaccard index," 2021, https://arxiv.org/abs/2110.09619#:~:text=Quantifying%20the%20similarity%20between%20two,several%20theoretical%20and%20applied%20problems.
[33] Flightaware, https://flightaware.com/, 2018.
[34] V. D. Blondel, J.-L. Guillaume, R. Lambiotte, and E. Lefebvre, "Fast unfold- ing of communities in large networks," *Journal of Statistical Mechanics: Theory and Experiment*, vol. 2008, no. 10, Article ID 10008, 2008.
[35] Di Jin, Z. Yu, P. Jiao et al., "A survey of community detection approaches: from statistical modeling to deep learning," *IEEE Transactions on Knowledge and Data Engineering*, p. 1, 2021.